

## Electron Spin Dynamics in a Self-Assembled Semiconductor Quantum Dot: The Limit of Low Magnetic Fields

I. A. Akimov, D. H. Feng, and F. Henneberger

*Institut für Physik, Humboldt Universität zu Berlin, Newtonstrasse 15, 12489 Berlin, Germany*

(Received 27 February 2006; published 3 August 2006)

Using the trion as an optical probe, we uncover novel electron spin dynamics in CdSe/ZnSe Stranski-Krastanov quantum dots. The longitudinal spin lifetime obeys an inverse power law associated with recharging processes in the dot ensemble. No hint at spin-orbit mediated spin relaxation is found. At very weak magnetic fields (<50 mT), electron spin dynamics related to the hyperfine interaction with the lattice nuclei is uncovered. A strong Knight field gives rise to nuclear ordering and formation of dynamical polarization on a 100- $\mu$ s time scale under continuous electron spin pumping. The associated spin transients are temperature robust and can be observed up to 100 K.

DOI: 10.1103/PhysRevLett.97.056602

PACS numbers: 72.25.Fe, 72.25.Rb, 78.55.Et, 78.67.Hc

Utilization of the spin for information processing has initiated extensive research in recent years, both in basic science and technology [1]. Practical applications require long spin lifetimes to store and to manipulate the spin without losses. In this regard, the spin states in semiconductor quantum dots (QDs) have attracted much interest. Localization on the nanometer length scale strongly suppresses spin-orbit coupling that controls the spin dynamics in bulk semiconductors [2]. In sufficiently strong magnetic fields, spin lifetimes in the millisecond range have been observed [3,4]. Here, the spin states are Zeeman split, and the interaction with acoustic phonons defines the major contribution [5]. At weak or zero magnetic field, the hyperfine interaction of the electron with the nuclear moments of the lattice atoms sets an ultimate limit for the spin lifetime in QDs [6,7]. Recent experimental studies have addressed dynamical nuclear polarization in QDs [8–10] and/or the inhomogeneous decay in spin ensembles [11–13]. However, the specific scenario for the spin transfer from the electron to the nuclear system as well as its dynamics and time scale has not yet been elaborated.

In this Letter, we report on measurements of the electron spin dynamics in Stranski-Krastanov QD structures. In the context of hyperfine interaction, II-VI QDs deserve attention. The strength of this interaction is characterized by the hyperfine constant  $A$  of the unit cell, the isotope abundance  $a$ , and the number of atoms  $N_L$  effectively seen by the electron. In the prototype CdSe/ZnSe structure, low natural abundance ( $a_{\text{Cd}} = 25\%$ ,  $a_{\text{Se}} = 8\%$ ) and a small value of  $A$ , related to the  $1/2$  isospin, make the Overhauser field  $B_N \sim aA$  acting on the electron by 1 to 2 orders of magnitudes smaller than in its III-V counterparts. On the other hand, the volume size is as little as  $50 \text{ nm}^3$ . Therefore, while  $N_L = 10^5$ – $10^6$  in typical III-V QDs, this number is reduced to a few 1000 in CdSe/ZnSe [14]. The hyperfine Knight field by which the electron acts on an individual nuclear spin scales like  $A/N_L$ . Thus, despite a small  $A$ , the role of the Knight field can be even stronger than in (In, Ga)As/GaAs.

The experimental concept of our study is based on the trion excitation in negatively charged QDs. The trion singlet ground state consists of two electrons with antiparallel spins and a single hole defining the total trion spin projection of  $\pm 3/2$ . Angular momentum conservation gives rise to circularly polarized optical transitions as schematized in Fig. 1(a). Hence, selective pumping, say, with photons of  $\sigma^+$  orientation, addresses only spin-up electrons. The resultant spin-up trions can radiatively recombine via the same channel or, after hole spin flip, by emitting  $\sigma^-$  photons and creating spin-down electrons. In this way, a nonequilibrium spin occupation with more spin-down than spin-up electrons is established. Now, switching from  $\sigma^+$  to  $\sigma^-$  excitation, the opposite scenario is started, ending up with a reversed spin occupation. Time resolving the associated emission change thus provides a direct optical monitor of the electron spin transients.

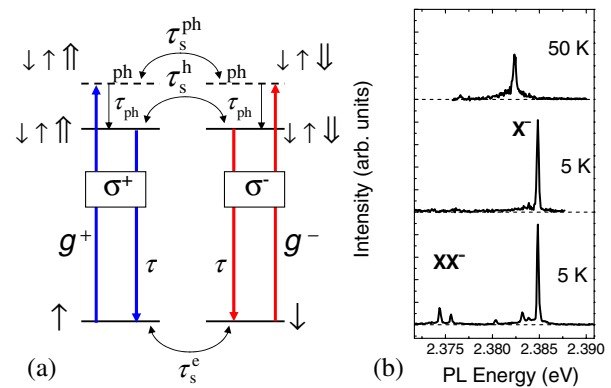


FIG. 1 (color online). (a) Optical transitions of a negatively charged QD.  $\uparrow, \downarrow$ , electron spin;  $\uparrow, \downarrow$ , hole spin;  $\tau, \tau_{\text{ph}}$ , lifetime of the trion ground- and LO-polaron state (labeled with ph), respectively;  $\tau_s^{\text{ph}}, \tau_s^{\text{h}}, \tau_s^{\text{e}}$ , spin-flip time of hole and electron, respectively;  $g^{\pm}$ , optical generation rates. (b) PL spectra of a single negatively charged QD under nonresonant (488 nm, bottom curve) and quasiresonant trion-polaron (514 nm, middle and top curves) excitation. Temperature as indicated.

The CdSe/ZnSe QD structures are grown by molecular beam epitaxy [14]. ZnSe is natively *n*-type so that a part of the CdSe QDs is negatively charged, even without intentional doping. In order to study individual QDs, mesa structures with an area down to  $100 \times 100 \text{ nm}^2$  are fabricated. Single mesas are optically selected by a microscope in a confocal arrangement with the propagation direction of incident and emitted light parallel to the [001] growth axis (*z* axis). The sample is mounted in a He-flow cryostat of variable temperature placed in a superconductive coil capable of magnetic fields  $B \leq 5 \text{ T}$  along *z* axis (Faraday geometry). Typical steady-state photoluminescence (PL) spectra of a single negatively charged QD under excitation with an Ar<sup>+</sup> laser are depicted in Fig. 1(b). Under nonresonant pumping in the energy continuum of the wetting layer (lowest curve), the characteristic double-line feature of the charged biexciton recombination ( $XX^-$ ) becomes visible, confirming that the QD is occupied with a single resident electron [15]. The first electron-excited trion state is a triplet with one of the electrons in the *p* shell and total electron spin projection of  $0, \pm 1$ . Involvement of the triplet state opens extra electron spin relaxation channels not related to the resident carrier and has thus to be avoided. In the measurements reported below, the QDs are hence quasiresonantly excited in a polaronlike mixed phonon-trion states, situated 1-LO-phonon energy above the trion singlet ground state. The triplet state is high-energy shifted from this position by about 80–100 meV and thus clearly separated [15]. Under these excitation conditions, a single line ( $X^-$ ) associated with the trion ground state is solely present in the PL spectra [upper curves in Fig. 1(b)].

In order to record the spin transients, the linear polarization of the excitation laser is modulated between two orthogonal states at frequencies ranging from  $f = 1 \text{ kHz}$  to 1 MHz by switching a Pockels cell with a rise time of 20 ns. Quarter- or half-wave plates convert this modulation in a respective series of circularly counter- or linearly cross-polarized excitation periods, or—when placed in the path of the PL—provide polarization selectivity in detection. The PL signal is dispersed in a double monochromator with a linear dispersion of 0.48 nm/mm and detected by a photomultiplier tube in conjunction with a multiscaler photon counting unit with an overall time resolution of 5 ns.

Single-dot PL transients recorded at the trion line under periodic circular polarization switching of the excitation are summarized in Fig. 2. The detection is always in  $\sigma^+$  mode. As discussed above,  $\sigma^+$  pumping aligns the electron spin increasingly down, decreasing the absorption of the excitation photons and hence the PL signal. Exactly this is seen in experiment. The transients are characterized by an amplitude  $\Delta I$ , defined as the difference between the signal level at the beginning and the end of the excitation period and a response time  $\tau_R$  taken at the  $1/e$  point of the signal decay. For  $\sigma^-$  excitation, the PL signal behaves qualitatively the same; however, the overall level is markedly

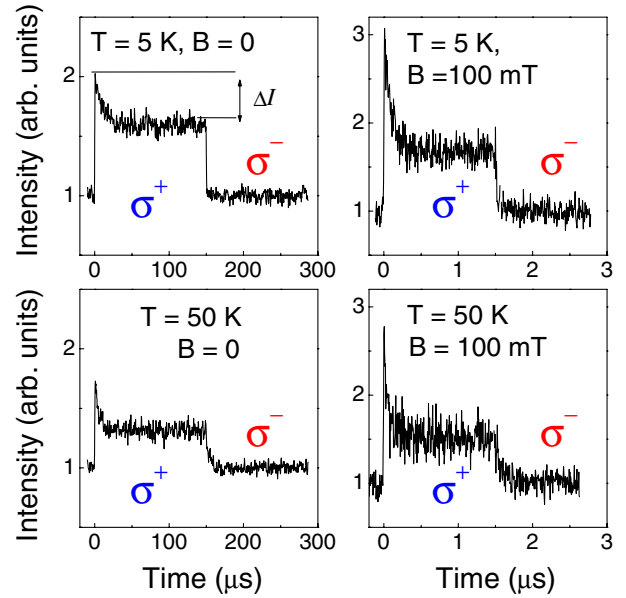


FIG. 2 (color online). Single QD electron spin transients under polarization switching excitation at zero ( $2 \text{ kW/cm}^2$ ) and weak external magnetic field  $B$  ( $200 \text{ W/cm}^2$ ) for low and moderate temperature  $T$ ; signal detection is in  $\sigma^+$  polarization. Note the different modulation rates in the left- and right-hand side panels and that the switching of the excitation polarization is instantaneous on both time scales.

smaller, indicating that the trion recombines predominantly along the arm in Fig. 1(a) where it has been excited. Detection in  $\sigma^-$  polarization provides identical results, only with the role of  $\sigma^+$  and  $\sigma^-$  excitation reversed.

At zero magnetic field, the response is slow and  $\tau_R$  on a 100- $\mu\text{s}$  time scale. Application of a weak longitudinal magnetic field of only a few 10 mT changes the picture dramatically. The amplitude of the slow transient increasingly disappears, while a fast component with roughly 3 orders of magnitude shorter response time emerges. Above  $B = 50 \text{ mT}$ , only the short transient is present. Another striking finding is that the response times are power dependent (see Fig. 3). This is most distinct for the short component that follows over 2 orders of magnitude very closely an inverse power law, while its amplitude stays practically constant. The slow component is also slightly sped up, but the amplitude increases with excitation power. The scenario is quite robust against temperature. Amplitude as well as response time only smoothly decrease from 5 to 50 K. In ensemble measurements with better signal-to-noise ratio, spin dynamics of the above type has even been resolved up to 100 K.

In order to translate the PL data into the underlying electron spin transients, one has to consider the Master equation for the density matrix with the generation, recombination, and relaxation rates given in Fig. 1(a). The lifetime  $\tau$  of the trion ground state is about 500 ps and the hole spin-flip time  $\tau_s^h \sim 10 \text{ ns}$  [16]. The times  $\tau_{\text{ph}}$  and  $\tau_s^{\text{ph}}$  of the trion-LO-polaron state are certainly shorter. That is, on the

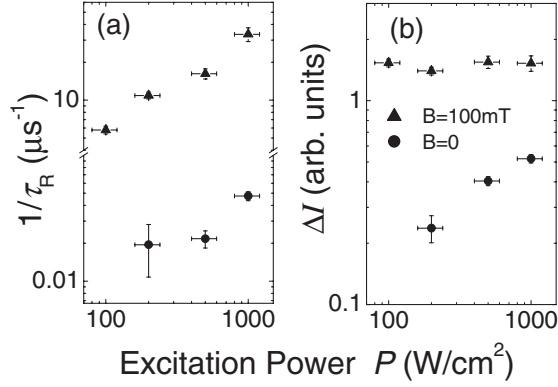


FIG. 3. Power dependence of single QD spin transients ( $T = 5$  K). (a) Inverse response time  $\tau_R$  and (b) switching amplitude  $\Delta I$ : triangles, fast component,  $B = 100$  mT,  $f = 333$  kHz; dots, slow component,  $B = 0$ ,  $f = 3.33$  kHz.

time scale of the experiment, the occupations of the trion states follow adiabatically the much slower electron spin dynamics. The emission from the QD is proportional to the trion ground-state occupation and a straightforward calculation yields then for the PL signal in  $\sigma^+$  detection  $I^\pm \propto (1 \pm Q)(1/2 \pm S_z)g^\pm$ , where  $\pm$  refers to  $\sigma^\pm$  excitation ( $g^\pm = g$ ) and  $S_z$  is the  $z$  projection of the average electron spin  $\vec{S}$ . The transients in Fig. 2 hence reflect directly the time evolution of the spin polarization of a single electron [17]. The parameter  $Q = \tau_s^{\text{ph}} \tau_s^h / (\tau_{\text{ph}} + \tau_s^{\text{ph}})(\tau + \tau_s^h) \in [0, 1]$  combines all lifetimes in the optically excited states and  $(1 - Q)$  is the fraction of trions driven into the other arm of the transition scheme. The weak low-temperature signal in counterpolarized excitation-detection mode, making the switching hardly observable, signifies that  $Q$  is close to 1. The signal growth, relative to copolarized mode, at higher temperatures is consistent with a shortening of the hole spin-flip time [16].

Assuming that the electron is subjected to an effective magnetic field creating a precession vector  $\vec{\Omega}$ , the dynamics of the average spin is described by the standard equation  $\dot{\vec{S}} = \vec{G} - \vec{R}(\vec{S}) + \vec{\Omega} \times \vec{S}$ . Specifically, for the present excitation scheme, the generation and relaxation rates are given by  $\vec{G} = (0, 0, \mp \frac{1}{4}[1 - Q]g)$ , for  $\sigma^\pm$  photons, and  $\vec{R} = (S_x/\tau_2^e, S_y/\tau_2^e, S_z[\frac{1}{2}(1 - Q)g + 1/\tau_1^e])$ , respectively. The power-dependent part of  $\vec{R}$  ensures  $|S_z| \leq 1/2$ ;  $\tau_1^e$  and  $\tau_2^e$  are the longitudinal and transverse spin lifetime, respectively.  $\vec{\Omega}$  is constituted by the external and the nuclear hyperfine field. An external field of some 10 mT is sufficient to outrange the nuclear contribution, and as a consequence of  $\vec{B} \parallel \vec{G}$ , the longitudinal part of the spin relaxation is predominant. The experimental power dependence reveals a characteristic spin-flip scenario for self-assembled QDs where the QD captures an extra charge created in its environment as a concomitant of the direct optical excitation. For example, capture of a hole produces an exciton that radiatively recombines followed by recap-

ture of another electron. Recharging processes of that type have been previously documented by spin-independent measurements [18]. They limit the lifetime of the single-electron state itself, but also randomize the spin as the latter is undetermined when the QD recovers to single-electron occupation. Introducing  $1/\tau_1^e = Dg$  yields a power-independent steady-state spin  $|S_z| = (1 - Q)/[2(1 - Q) + 4D]$ , in full accord with the experiment. We estimate  $1/Dg \sim 400$  ns at an excitation intensity of  $100 \text{ W}/\text{cm}^2$ . Decreasing the excitation rate down to a level at which the PL signal disappears in the noise floor, spin-flip times of about  $10 \mu\text{s}$  are found. However,  $\tau_R$  does not approach an offset value, demonstrating that the intrinsic spin lifetime due to spin-orbit coupling is significantly longer than  $10 \mu\text{s}$ .

The recharging processes are not affected by an external field of a few 10 mT. The 10–100  $\mu\text{s}$  transients at  $B = 0$  thus display a situation where the electron spin is in steady state, in the sense that  $\dot{\vec{S}} = \vec{0}$  holds. The decay of the PL signal displays now an increase of  $|S_z|$  as a result of a slowly increasing total (longitudinal and transverse) spin lifetime  $\tau_s^e$ . For  $(\Omega_z \tau_s^e)^2 \gg 1$ , it follows from the precession equation in steady state  $1/\tau_s^e = 1/\tau_1^e + \Theta^2/\tau_2^e$ . The parameter  $\Theta^2 = (\Omega_x^2 + \Omega_y^2)/\Omega_z^2$  measures the order in the nuclear system, with  $\Theta^2 = 2$  in a random configuration. The experimental data hence reveal an increasing nuclear ordering ( $\Theta^2 < 2$ ) under continuous electron spin pumping suggesting the formation of a nuclear polarization. At zero external field, the latter demands that the hyperfine Knight field  $B_e$ , acting here solely on the nuclei, exceeds the local field  $B_L$  created by the nuclear dipole-dipole interaction [19]. A detailed study of the Knight field requires account of its inhomogeneous nature, caused by the change of the electron wave function across the nuclear ensemble [7], and is beyond the scope of this work. Accepting  $B_e \sim (1/2\mu_I)(A/N_L)S_z$  as an estimate and using for  $\mu_I \approx -0.6\mu_N$  the nuclear moment of the  $\text{Cd}^{111,113}$  isotopes and  $A \approx -10 \mu\text{eV}$ , it follows  $B_e \sim 300S_z/N_L$  T, while  $B_L$  is in the sub-mT range. Thus, in view of the relatively small  $N_L$ ,  $B_e$  overcomes  $B_L$  already for moderate electron spin polarization. The power dependencies of the slow transients in Fig. 3 are then readily explained: a larger spin pumping rate  $g$  produces a stronger  $B_e$ , which in turn makes  $\Theta^2$  smaller, establishing a longer  $\tau_s^e$  in a shorter time  $\tau_R$ .

The existence of a nuclear polarization is confirmed by a distinct asymmetry of the slow electron spin transients with regard to the direction of the external magnetic field. The data in Fig. 4, selectively verified on a single-dot level, are taken from ensemble measurements allowing for shorter integration times. An external field decreases in general the amplitude as the lifetime change contributed by the nuclear field declines. However, that decrease will be steeper when  $B$  and the Overhauser field compensate resulting in a shorter  $\tau_s^e$  and keeping thus the electron spin along the transient small. Correspondingly,  $1/\tau_R$  becomes smaller in

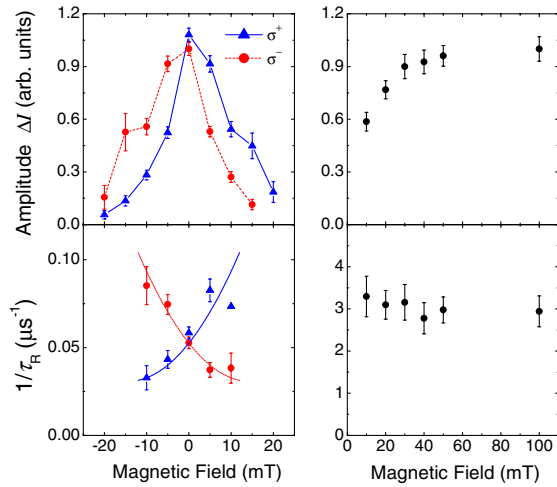


FIG. 4 (color online). Left panel: Spin amplitude and inverse response time versus magnetic field for the slow component ( $f = 3.33$  kHz). Right panels: Fast component ( $f = 333$  kHz). The data are extracted from transients recorded in copolarized excitation-detection mode.  $\sigma^\pm$  denotes the polarization in detection. The lines are guides to the eye.  $T = 50$  K.

this field direction consistent with the power dependence of Fig. 3: the rate at which the nuclear polarization is established decreases when the electron spin polarization is weak. The asymmetries depicted in Fig. 4 are consistent with a negative value of  $A$  anticipated for  $\mu_I < 0$ . For example,  $\sigma^-$  excitation means  $S_z > 0$  and for the average nuclear spin  $I_z > 0$  but  $B_N < 0$ .  $B_e$  is oppositely directed to  $B_N$  and the shoulders on the smoothly decaying wings of the amplitude are likely a direct signature of the Knight field. In marked contrast, no asymmetry is observed for the fast component. The data in the right panel of Fig. 4 are recorded in a rapid ( $3 \mu\text{s}$ ) modulation regime, excluding creation of a nuclear polarization. Thus, when approaching zero field, the transverse relaxation associated with the random nuclear configurations in the QD ensemble destroys an increasing part of the spin polarization on a time scale  $1/\sqrt{\langle \Omega^2 \rangle} \sim \sqrt{aN_L} \hbar / (aA) \sim 5$  ns [6,7] below our experimental resolution, while the rest decays with the longitudinal lifetime. This is exactly seen in the experiment: the amplitude drops down whereas the response time stays practically constant.

In conclusion, we have uncovered the specific scenario of the electron spin dynamics in self-assembled QDs. At magnetic fields far below the onset of a phonon-mediated spin flip, purely longitudinal spin relaxation as a result of recharging processes, representing an inherent feature of the Stranski-Krastanov morphology, is observed. The inversely power-dependent relaxation times reach a few microseconds at low excitation in the present QD structures. The intrinsic spin-orbit time of an isolated QD is significantly longer. Spin-induced nuclear ordering and

formation of a nuclear polarization at zero external magnetic field is observed. The time needed for the formation of an appreciable dynamical polarization is on the sub-ms scale and hence much shorter than for bulk semiconductors, probably caused by the substantially longer electron correlation time in QDs. The data are qualitatively well understood in a mean-field frame; the true statistical state of the nuclear system cannot, however, be deduced from the above measurements and deserves further investigation. Spin dynamics of this type is observed up to 100 K signifying that the nuclear moments are decoupled from the lattice up to elevated temperatures.

This work was supported by the Deutsche Forschungsgemeinschaft within Project No. He 1939/18-1.

- [1] See, e.g., A. Žutic, J. Fabian, and S. Das Sarma, *Rev. Mod. Phys.* **76**, 323 (2004), and references therein.
- [2] A. V. Khaetskii and Yu. V. Nazarov, *Phys. Rev. B* **61**, 12 639 (2000).
- [3] J. M. Elzerman *et al.*, *Nature (London)* **430**, 431 (2004).
- [4] M. Kroutvar *et al.*, *Nature (London)* **432**, 81 (2004).
- [5] A. V. Khaetskii and Yu. V. Nazarov, *Phys. Rev. B* **64**, 125316 (2001); L. M. Woods, T. L. Reinecke, and Y. Lyanda-Geller, *Phys. Rev. B* **66**, 161318(R) (2002).
- [6] I. A. Merkulov, A. L. Efros, and M. Rosen, *Phys. Rev. B* **65**, 205309 (2002).
- [7] A. V. Khaetskii, D. Loss, and L. Glazman, *Phys. Rev. Lett.* **88**, 186802 (2002); *Phys. Rev. B* **67**, 195329 (2003).
- [8] A. S. Bracker *et al.*, *Phys. Rev. Lett.* **94**, 047402 (2005).
- [9] R. Oulton *et al.*, cond-mat/0505456; C. W. Lai *et al.*, cond-mat/0512269.
- [10] M. Ikezawa *et al.*, *Phys. Rev. B* **72**, 153302 (2005).
- [11] M. V. Gurudev Dutt *et al.*, *Phys. Rev. Lett.* **94**, 227403 (2005).
- [12] J. A. Gupta *et al.*, *Phys. Rev. B* **66**, 125307 (2002).
- [13] P. F. Braun *et al.*, *Phys. Rev. Lett.* **94**, 116601 (2005).
- [14] D. Litvinov *et al.*, *Appl. Phys. Lett.* **81**, 640 (2002); A. Hundt *et al.*, *Phys. Rev. B* **69**, 121309(R) (2004).
- [15] I. A. Akimov *et al.*, *Appl. Phys. Lett.* **81**, 4730 (2002); *Phys. Status Solidi A* **201**, 412 (2004); *Phys. Rev. B* **71**, 075326 (2005).
- [16] T. Flissikowski *et al.*, *Phys. Rev. B* **68**, 161309(R) (2003).
- [17] The number of this polarization can be extracted from the data. However, heavy-light hole coupling [see A. V. Koudinov *et al.*, *Phys. Rev. B* **70**, 241305(R) (2004)] spoiling the circular polarization selectivity of the two arms in the trion transition scheme has to be accounted for. A detailed discussion goes beyond the scope of this Letter and will be given elsewhere. We find maximum electron spin polarization degrees of about  $2S_z = 0.5$ .
- [18] C. Santori *et al.*, *Phys. Rev. B* **69**, 205324 (2004).
- [19] V. G. Fleisher and I. A. Merkulov, in *Optical Orientation*, edited by F. Meier and B. P. Zakharchenya (North Holland, Amsterdam, 1984), p. 173.